Synthesis and Stereochemical Rearrangements of Complexes Containing the Fe–S_6 Core

L. H. Pignolet,[1] R. A. Lewis,[1] and R. H. Holm*

Contribution from the Department of Chemistry, Massachusetts Institute of Technology, Cambridge, Massachusetts 02139.
Received June 18, 1970

Abstract: Anaerobic reaction between bis(N,N-disubstituted-dithiocarbamato)iron(II) complexes and bis(perfluoromethyl)-1,2-dithietene in tetrahydrofuran solution has resulted in the synthesis of a new class of complexes, designated as $Fe(R_1R_2dtc)_2(tfd)$, which contain the Fe–S_6 core. These complexes are involved in a singlet–triplet spin-state equilibrium and manifest isotropically shifted nmr spectra. Studies of these spectra in dichloromethane solution over the range −100–90° have led to the detection of two intramolecular rearrangement reactions differing by *ca.* 10^3 in rate at 25°. Proton and fluorine spectra of $Fe(MePh(dtc))_2(tfd)$ serve to identify the low-temperature process (detectable below *ca.* −5°) as inversion of the molecular configuration. The high-temperature process is assigned as C–N bond rotation. Comparison of preexchange lifetimes and activation parameters, obtained by line-shape analysis, indicates that these low- and high-temperature processes are the same for symmetrically substituted complexes ($R_1 = R_2$) whose pmr spectra do not necessarily distinguish between inversion and bond rotation. Constraints placed upon the pathway for inversion by the spectra of $Fe(MePh(dtc))_2(tfd)$ have permitted its identification with considerable certainty. Analysis of bond-rupture and twist pathways has shown that only a twist motion about the pseudothreefold axis is sensibly consistent with the nmr spectral constraints. Correlation diagrams for rearrangements of an $M(A–A')_2(B–B)$ complex *via* trigonal-bipyramidal, square-pyramidal, and trigonal-prismatic transition states have been derived and are presented. The present work provides the best available evidence for the operation of a twist mechanism in the rearrangement reactions of chelates. The physical basis for this mechanism is believed to be the significant distortion toward an effective trigonal-prismatic configuration found in the structure of crystalline $Fe(Et_2(dtc))_2(tfd)$. The preparation of analogous $M(R_1R_2dtc)_2(tfd)$ complexes with M = Ru, Mn, and Co is also reported.

Mono- and polynuclear complexes containing Fe–S_n cores (n = 4, 5, or 6) are currently commanding much attention because of their frequently unusual electronic and structural properties and their possible, although as yet unestablished, relevance to the iron–sulfur coordination units in nonheme iron proteins. Chelates derived from 1,1- and 1,2-dithio ligands have been characterized in some detail, and those of the Fe–S_6 type are pertinent to the present investigation. 1,1-Dithio complexes[2] include the trischelates of dithiocarbamates,[3,4] xanthates,[5] thioxanthates,[6,7] dithiophosphates,[5] and dithiocarboxylates;[8,9] 1,2-dithio species are principally of the tris(dithiolene) variety.[10] The most conspicuous properties of the former group are the widespread occurrence of the doublet–sextet spin equilibrium,[3–5,7,11] well-resolved isotropically shifted nmr spectra[12–14] whose temperature dependencies reveal this equilibrium,[13,14] and structures which are distorted toward a trigonal-prismatic geometry.[15,16] Important features of the latter group are the triplet ground state found in dianionic complexes and the existence of electron-transfer series whose members are interrelated by one-electron redox processes.[10]

In the course of investigating oxidative addition reactions of the air-sensitive bis(N,N-disubstituted-dithiocarbamato)iron(II) complexes with ligating sulfur compounds, a new series of Fe–S_6 complexes has been prepared which possess certain of the general properties of the aforementioned 1,1- and 1,2-dithio species. Treatment of the iron(II) complexes with bis(perfluoromethyl)-1,2-dithietene,[17] $S_2C_2(CF_3)_2$, results in the formation of $Fe(S_2CNR_1R_2)_2[S_2C_2(CF_3)_2]$, hereafter designated as $Fe(R_1R_2dtc)_2(tfd)$. As reported recently,[18] members of this series of complexes manifest three properties not previously encountered in the *same* molecular species: (i) magnetic properties consistent with a singlet–triplet spin equilibrium in the crystalline state and in solution; (ii) redox properties indicative of a three-membered electron transfer series with the $0 \rightleftharpoons -1$ interconversion electrochemically reversible; (iii) stereochemical mobility of a ligand structural portion (restricted rotation about the S_2C–N bonds) and of the overall molecular configuration itself (inversion), with the detection of both processes facilitated by accentuated chemical shift differences due to isotropic interactions.[19] This article describes the syn-

(1) National Institutes of Health Postdoctoral Fellow, 1969–1970.
(2) For a review, *cf.* D. Coucouvanis, *Progr. Inorg. Chem.*, 11, 233 (1970).
(3) A. H. White, E. Kokot, R. Roper, H. Waterman, and R. L. Martin, *Aust. J. Chem.*, 17, 294 (1964).
(4) A. H. Ewald, R. L. Martin, I. G. Ross, and A. H. White, *Proc. Roy. Soc., Ser. A*, 280, 235 (1964).
(5) A. H. Ewald, R. L. Martin, E. Sinn, and A. H. White, *Inorg. Chem.*, 8, 1839 (1969).
(6) D. Coucouvanis, S. J. Lippard, and J. A. Zubieta, *J. Amer. Chem. Soc.*, 91, 761 (1969); 92, 3342 (1970).
(7) A. H. Ewald and E. Sinn, *Aust. J. Chem.*, 21, 927 (1968).
(8) E. Cervone, F. D. Camassei, M. L. Luciani, and C. Furlani, *J. Inorg. Nucl. Chem.*, 31, 1101 (1969).
(9) D. Coucouvanis and S. J. Lippard, *J. Amer. Chem. Soc.*, 91, 307 (1969).
(10) J. A. McCleverty, J. Locke, E. J. Wharton, and M. Gerloch, *J. Chem. Soc. A*, 816 (1968); E. J. Wharton and J. A. McCleverty, *ibid., A*, 2258 (1969); E. I. Steifel, L. E. Bennett, Z. Dori, T. H. Crawford, C. Simo, and H. B. Gray, *Inorg. Chem.*, 9, 281 (1970).
(11) R. L. Martin and A. H. White, *Transition Metal Chem.*, 4, 113 (1968).
(12) E. E. Zaev, S. V. Larionov, and Yu. N. Molin, *Dokl. Chem.*, 168, 480 (1966).
(13) R. M. Golding, W. C. Tennant, C. R. Kanekar, R. L. Martin, and A. H. White, *J. Chem. Phys.*, 45, 2688 (1966).
(14) R. M. Golding, W. C. Tennant, J. P. M. Bailey, and A. Hudson, *ibid.*, 48, 764 (1968).
(15) B. F. Hoskins and B. P. Kelly, *Chem. Commun.*, 1517 (1968).
(16) B. F. Hoskins and B. P. Kelly, *ibid.*, 45 (1970).
(17) C. G. Krespan, *J. Amer. Chem. Soc.*, 83, 3434 (1961).
(18) L. H. Pignolet and R. H. Holm, *ibid.*, 92, 1791 (1970).

Table I. Characterization Data for Bis(N,N-disubstituted-dithiocarbamato)bis(perfluoromethyl)-1,2-dithiolene Complexes, $M(R_1R_2dtc)_2(tfd)$

M	R_1	R_2	Mp, °C[a]	Calcd, % C	Calcd, % H	Calcd, % N	Calcd, % S	Found, % C	Found, % H	Found, % N	Found, % S
Fe	Me	Me	*b*	22.98	2.32	5.36	36.82	23.22	2.32	5.46	36.83
Fe	Et	Et	184–185	29.10	3.50	4.84	33.24	29.18	3.40	4.74	33.36
Fe	Me	CH_2Ph	155–156	39.17	2.99	4.15		38.69	2.93	4.32	
Fe[c]	Me	Ph	133–135	34.47	2.48	3.80		34.53	2.37	3.50	
Fe	$(CH_2)_4$		214–215	29.27	2.80	4.88	33.48	29.27	3.00	5.02	32.66
Fe	$(CH_2)_5$		*b*	31.96	3.34	4.66	32.00	31.68	3.47	4.77	31.70
Ru	Me	Me	262	21.16	2.13	4.93	33.89	21.17	2.17	4.92	33.30
Ru	Et	Et	201–202	26.96	3.23	4.49	30.84	26.93	3.19	4.47	30.51
Ru[d]	Me	Ph	160–175[e]	29.83	1.91	3.31		29.40	1.96	3.37	
Co	Me	Me	*b*	22.86	2.30	5.33		22.70	2.26	5.13	
Co	Et	Et	135–136	28.91	3.47	4.82	33.08	29.10	3.43	4.77	33.24
Mn	Et	Et	155–157	29.11	3.49	4.85	33.30	29.09	3.42	4.81	33.71

[a] Uncorrected, determined *in vacuo*. [b] Decomposes at >200°. [c] Dichloromethane monosolvate. [d] Carbon tetrachloride monosolvate. [e] Decomposition.

thesis of members of this series and of analogous manganese, ruthenium, and cobalt species, and a detailed investigation of property iii of the iron complexes. Electronic and redox properties will be reported in full upon completion of work in progress.[20]

Experimental Section

Preparation of Compounds. Characterization data for the complexes $M(R_1R_2dtc)_2(tfd)$ prepared in this work are presented in Table I. Bis(perfluoromethyl)-1,2-dithietene was obtained by the method of Krespan.[17]

Iron Complexes. Bis(*N,N*-diethyldithiocarbamato)bis(perfluoromethyl)dithioleneiron, $Fe(Et_2(dtc))_2(tfd)$. Bis(*N,N*-diethyldithiocarbamato)iron(II)[21] (2.7 g, 7.7 mmol) was dissolved in freshly distilled, thoroughly degassed tetrahydrofuran (150 ml) to give a yellowish-red solution. Rigorous exclusion of oxygen is essential in this and the next several steps to prevent formation of tris(*N,N*-diethyldithiocarbamato)iron(III), $Fe(Et_2(dtc))_3$. To this solution 1.7 g (7.7 mmol) of bis(perfluoromethyl)-1,2-dithietene in 10 ml of oxygen-free tetrahydrofuran was added. An immediate darkening occurred. The solution was stirred at room temperature under nitrogen for several hours and the solvent removed under reduced pressure. In the presence of air the black residue was extracted with dry dichloromethane. *n*-Heptane was added to the deep red-brown extract solution and the product was crystallized by slow evaporation of the solvent to afford 2.1 g of shiny black crystals. Several recrystallizations from *n*-heptane–dichloromethane were required to give a product which was pure by tlc on silica gel and by elemental analysis. On several occasions a product was obtained by extraction which contained some $Fe(Et_2(dtc))_3$. This impurity was identified by its pmr spectrum[13] and separated from the desired product by chromatography on a silica gel column. The pure complex was obtained from the benzene eluate of the rapidly moving reddish-brown band.

$Fe(R_1R_2dtc)_2(tfd)$ complexes ($R_1 = R_2 = Me$; $R_1, R_2 = (CH_2)_4$ and $(CH_2)_5$; and $R_1 = Me$, $R_2 = CH_2Ph$ or Ph) were prepared by a procedure analogous to that used for $Fe(Et_2(dtc))_2(tfd)$. In these cases, however, the bis(dithiocarbamato)iron(II) complexes were not appreciably soluble in tetrahydrofuran and suspensions were used. Addition of the dithietene produced deep red-brown solutions after several hours of stirring. Yields and appearance of products were similar to $Fe(Et_2(dtc))_2(tfd)$. Spectral properties of $Fe(Et_2(dtc))_2(tfd)$ follow: ir (mull) 2975 (w, $\nu_{as}CH_3$), 2930 (w, ν_{as} CH_2), 2865 (vw), 1620 (vw), 1560 (w, sh), 1510 (s, C···N), 1450 (sh $\delta_{as}CH_3$), 1440 (s, CH_2 scissor), 1380 (m, δ_sCH_3), 1350 (m), 1300 (m), 1278 (s), 1270–1220 (s, br), 1210 (sh), 1185–1165 (s, br), 1160–1135 (s, br), 1095 (w), 1075 (m), 995 (w), 935 (vw), 910 (vw), 850 (m) 780 (m), 725 (m), 720 (sh, w), 685 (m), 580 cm^{-1} (w); electronic, spectrum ($CHCl_3$) [λ_{max}, cm^{-1} (ϵ)] 11,400 (sh, 170), 15,200 (1700), 18,500 (1970), 26,300 (sh, 6550), 29,100 (9080), 35,700 (sh, 27,700), 38,100 (33,800).

Bis(*N,N*-diethyldithiocarbamato)iron(II), $Fe(Et_2(dtc))_2$. This complex, which is typical of those used in the reactions with bis(perfluoromethyl)-1,2-dithietene, has been previously reported[21] but not completely characterized. An extremely air sensitive chocolate-brown impure powder was isolated from the reaction mixture of ferrous sulfate heptahydrate (5.0 g, 18 mmol) and the sodium diethyldithiocarbamate (8.1 g, 36 mmol) in 200 ml of thoroughly degassed water. This powder was transferred under nitrogen to a Soxhlet extractor and was extracted with degassed acetone for 24 hr, after which red needles appeared. Filtration and vacuum drying yielded ~5 g of pure product, mp *ca.* 230° dec. *Anal.* Calcd for $C_{10}H_{20}N_2S_6Fe$: C, 34.08; H, 5.72; N, 7.95; S, 36.40. Found: C, 33.91; H, 5.55; N, 7.86; S, 36.40.

Ruthenium Complexes. Bis(*N,N*-diethyldithiocarbamato)bis(perfluoromethyl)dithioleneruthenium, $Ru(Et_2(dtc))_2(tfd)$. Bis(diethyldithiocarbamato)carbonylruthenium(II)[22] (2.5 g, 5.3 mmol) was slurried in 100 ml of freshly distilled tetrahydrofuran and 1.42 g (6.3 mmol) of bis(perfluoromethyl)-1,2-dithietene in 10 ml of tetrahydrofuran added under nitrogen. The mixture was stirred and heated at reflux under nitrogen for 15 hr, and the intensely colored red-violet solution filtered in air. The solvent was removed from the filtrate on a rotary evaporator and the residue was dissolved in hot carbon tetrachloride and filtered. The product was precipitated with *n*-heptane as a violet crystalline solid (1.95 g). It was further purified by recrystallization from this solvent mixture, followed by chromatography on Florisil (benzene eluent), and, finally, by recrystallization from benzene–*n*-heptane. The product was homogeneous by tlc on silica gel when eluted with benzene: electronic spectrum ($CHCl_3$) [λ_{max}, cm^{-1} (ϵ)] 8700 (220), 12,000 (sh, 950), 17,700 (4140), 19,900 (sh, 3230), 31,300 (sh, 11,300), 35,800 (sh, 25,200), 39,500 (sh, 33,700).

$Ru(Me_2(dtc))_2(tfd)$ and $Ru(MePh(dtc))_2(tfd)$ were prepared in a similar manner from the appropriate carbonyl precursors. The former was recrystallized from *n*-hexane–dichloromethane and the latter from carbon tetrachloride.

Cobalt Complexes. Bis(*N,N*-diethyldithiocarbamato)bis(perfluoromethyl)dithiolenecobalt, $Co(Et_2(dtc))_2(tfd)$. Cobalt chloride hexahydrate (1.1 g, 4.4 mmol) and bis(perfluoromethyl)-1,2-dithietene (1.0 g, 4.4 mmol) were combined in 150 ml of tetrahydrofuran, freshly distilled from lithium aluminum hydride, and the resultant blue solution was thoroughly degassed. Sodium *N,N*-diethyldithiocarbamate (2.0 g, 8.9 mmol) in 25 ml of degassed, dry tetrahydrofuran was added by a syringe and the brown reaction mixture stirred for 3 hr under a pure nitrogen atmosphere. The mixture was filtered in air and the precipitate, primarily tris(*N,N*-diethyldithiocarbamato)cobalt(III), was washed with tetrahydrofuran. The combined filtrate and wash was concentrated on a rotary evaporator to an oil, which was triturated with *n*-hexane in order to remove some brown impurity. The residue was dissolved in dichloromethane and filtered and the crude product was precipitated by addition of *n*-heptane. It was chromatographed on Florisil using benzene as the eluent. A rapidly moving brown band

(19) R. H. Holm, *Accounts Chem. Res.*, 2, 307 (1969).

(20) L. H. Pignolet, R. A. Lewis, A. Gold, J. F. Weiher, and R. H. Holm, unpublished investigations.

(21) J. P. Fackler, Jr., and D. G. Holah, *Inorg. Nucl. Chem. Lett.*, 2, 251 (1966).

(22) J. V. Kingston and G. Wilkinson, *J. Inorg. Nucl. Chem.*, 28, 2709 (1966).

Table II. Proton and Fluorine Chemical Shifts of $M(R_1R_2dtc)_2(tfd)$ Complexes

Complex	Solvent	Temp, °C	^1H shifts,[a] ppm	^{19}F shifts,[b] ppm
$Fe(Me_2(dtc))_2(tfd)$	CD_2Cl_2	−92[k]	CH_3, −5.33, −5.90	*i*
		30	CH_3, −7.46	−17.46
$Fe(Et_2(dtc))_2(tfd)$	CD_2Cl_2	−92[k]	CH_2, −4.40, (−5.05[i]), 7.05; CH_3, −0.97, −1.58	*i*
		30	CH_2, −5.84, −7.60; CH_3, −1.31[c]	−20.78
$Fe[(CH_2)_4(dtc)]_2(tfd)$	CD_2Cl_2	30	α-CH_2, −12.70, −13.20; β-CH_2, −1.70	−19.72
$Fe[(CH_2)_5(dtc)]_2(tfd)$	CD_2Cl_2	−92[k]	α-CH_2, (−5.38[i]), −6.43, −7.23, −9.25	*i*
		30	α-CH_2, −7.94, −9.81; β-CH_2, −1.80; γ-CH_2, −2.80	−22.50
$Fe(Me,CH_2Ph(dtc))_2(tfd)$	CD_2Cl_2	30	CH_2, −6.09, −6.90; CH_3, −6.21	−14.63 (13°)
$Fe(MePh(dtc))_2(tfd)$	CD_2Cl_2	−92[k]	CH_3, −4.06, −4.15, −4.27, −4.38	*i*
		30	CH_3,[d] −5.77, −5.91; *o*-, *m*-H, −7.14, −7.62; *p*-H, −7.35	−14.46 (41°)
$Ru(Me_2(dtc))_2(tfd)$	CD_2Cl_2	30	CH_3, −3.23	−7.72
$Ru(Et_2(dtc))_2(tfd)$	CD_2Cl_2	30	CH_2,[e] −3.61, −3.63; CH_3, −1.18[c]	−7.82
$Ru(MePh(dtc))_2(tfd)$	$CDCl_3$	15	CH_3,[f] −3.59, −3.69; *o*-, *m*-, *p*-H, −7.37[h]	−7.66
$Co(Me_2(dtc))_2(tfd)$	$CDCl_3$	30	CH_3,[g] −1.24, −5.46	*i*
$Co(Et_2(dtc))_2(tfd)$	$CDCl_3$	30	CH_2,[g] −2.60, −4.70, −5.39; CH_3, −1.70, −1.87	*i*

[a] TMS internal standard. [b] $C_6H_5CF_3$ internal standard. [c] Triplet, J = 7.1 Hz. [d] 0°, signals coalesce at +13°. [e] Quartets, J = 7.1 Hz. [f] Signals coalesce at +40°. [g] Very broad signals. [h] Center of complex multiplet. [i] Not measured. [j] Partially obscured by $CHDCl_2$ signal. [k] Slow exchange conditions.

was collected, leaving a green band on the column. The brown eluate was concentrated and the product obtained as black crystals upon slow addition of *n*-hexane. The product (0.50 g, 20%) was found to be homogeneous by tlc on silica gel with benzene eluent: electronic spectrum ($CHCl_3$) [λ_{max}, cm^{-1} (ϵ)] 10,900 (1130), 17,350 (1260), 28,600 (sh, 13,400), 31,400 (34,400), 37,600 (34,000).

$Co(Me_2(dtc))_2(tfd)$ was prepared in an analogous manner and obtained as black needles upon recrystallization from *n*-hexane–dichloromethane.

Bis(diethyldithiocarbamato)bis(perfluoromethyl)dithiolenemanganese, $Mn(Et_2(dtc))_2(tfd)$. Manganese chloride tetrahydrate (1.0 g, 5.0 mmol) and sodium *N*,*N*-diethyldithiocarbamate (2.25 g, 10 mmol) were allowed to react under nitrogen in 125 ml of carefully degassed ethanol. To the resultant yellow slurry, which presumably contains bis(*N*,*N*-diethyldithiocarbamato)manganese(II),[21] 1.13 g (5.0 mmol) of bis(perfluoromethyl)-1,2-dithietene in 10 ml of degassed ethanol was added by means of a syringe. The reaction mixture, which immediately turned to brown-violet, was stirred for 2 hr at room temperature and then filtered. The black precipitate was dissolved in dichloromethane and the solution filtered to remove sodium chloride. Addition of *n*-hexane resulted in the formation of a crystalline solid, which was rapidly chromatographed on a Florisil column (wrapped with foil to prevent photodecomposition) using benzene as the eluent. Red-brown eluate (300–500 ml) was collected. Solvent was removed from the eluate and the residue was recrystallized under nitrogen from dry dichloromethane–*n*-heptane to yield the product (0.25 g, 9%) as small black needles. The compound is photosensitive, especially in solution, and unstable in moist air; it was stored under dry nitrogen in the dark: electronic spectrum (anaerobic $CHCl_3$ solution) [λ_{max}, cm^{-1} (ϵ)] 9750 (256), 15,400 (sh, 1300), 20,800 (sh, 5600), 25,300 (10,850), 33,900 (sh, 19,500), 37,500 (36,600).

Molecular Weights. Determinations were made in toluene solutions at 37° using a Mechrolab osmometer, benzil as calibrant, and concentrations of *ca.* 4×10^{-5} mol/g of solvent. *Anal.* Calcd for $Fe(Me_2(dtc))_2(tfd)$: mol wt, 523. Found: mol wt, 527. Calcd for $Fe(Et_2(dtc))_2(tfd)$: mol wt, 579. Found: mol wt, 575. Calcd for $Fe[(CH_2)_4(dtc)]_2(tfd)$: mol wt, 575. Found: mol wt, 590. Calcd for $Fe[(CH_2)_5(dtc)]_2(tfd)$: mol wt, 603. Found: mol wt, 587.

Nmr Measurements. Proton and fluorine spectra were recorded on a Varian HA-100 spectrometer equipped with a variable-temperature probe and an external oscillator. Chemical shifts were measured in the HA or HR mode of operation relative to TMS or perfluoromethyltoluene as internal standards. Temperatures were monitored by a thermocouple mounted in the probe, which was repeatedly calibrated with methanol or ethylene glycol,[23] and are accurate to ±1°. Kinetic studies were carried out in the HA operating mode at rf power levels well below saturation. *Ca.* 0.1 *M* solutions were prepared by weight in CD_2Cl_2 solvent, degassed, sealed in nmr tubes, and used immediately thereafter. Chemical shifts of the complexes at selected temperatures in CD_2Cl_2 or $CDCl_3$ solutions are set out in Table II; all shifts are downfield of the internal standards.

Kinetic Analysis. Stereochemical rearrangements of $Fe(R_1R_2dtc)_2(tfd)$ complexes in CD_2Cl_2 solutions were investigated by nmr measurements over the range −100–90°. Two rearrangement processes were detected for this group of complexes, each member of which clearly exhibited one process or both of them. Experimental observations and arguments presented in the text support assignments of the low- and high-temperature rearrangement processes to inversion of the absolute configuration of the complex and C–N bond rotation, respectively. The low-temperature process usually did not cause exchange broadening above *ca.* −5°, while a similar limit for the high-temperature process was *ca.* 80°. Kinetic analyses of the two processes were performed by a line-shape method. These processes were investigated in detail for the following complexes using the resonance signals indicated: low-temperature process $Fe(Me_2(dtc))_2(tfd)$, CH_3; $Fe(Et_2(dtc))_2(tfd)$, CH_3; high-temperature process $Fe(Et_2(dtc))_2(tfd)$, CH_2; $Fe[(CH_2)_5(dtc)]_2(tfd)$, α-CH_2; $Fe(MePh(dtc))_2(tfd)$, CH_3. Simulated spectra were calculated by a total line-shape analysis using the Whitesides–Lisle EXCNMR computer program,[24] which employs the methods developed by Kubo and Sack.[25] Each dynamic process was treated as a simple two-site exchange where environments A and B have identical populations and transverse relaxation times. The calculation of exchange-broadened line shapes for a given process requires line positions and widths for environments A and B in the absence of exchange broadening. These values were determined by appropriate extrapolations and comparisons to similar compounds not exhibiting the process in question. For two-site exchange only the chemical shift difference between A and B, $\Delta\nu$, and their respective line widths at half-height, $\Delta H_{1/2}$, are required. Because of the temperature-dependent paramagnetism of the complexes, certain empirical procedures were adopted to obtain reasonable values of $\Delta\nu$ and $\Delta H_{1/2}$. Given in Table III are values of $\Delta\nu$ of α-methylene protons used in analyzing the high-temperature processes of $Fe(Et_2(dtc))_2(tfd)$ and $Fe[(CH_2)_5(dtc)]_2(tfd)$. These values were determined by linear extrapolation of the slow-exchange shifts *vs.* $1/T$ up to 55° and by following the slight curvature observed for the dimethyl analog above 55°. Confidence in this procedure is gained from the observations that the slow-exchange shifts are linear *vs.* $1/T$ from −20 to 20° and the averaged resonance position in the fast-exchange region is that predicted by the extrapolation for both

(23) A. L. Van Geet, *Anal. Chem.*, 40, 2227 (1968).

(24) G. M. Whitesides and J. S. Fleming, *J. Amer. Chem. Soc.*, 89, 2855 (1967); J. B. Lisle, S.B. Thesis, Massachusetts Institute of Technology, 1968.

(25) R. Kubo, *Nuovo Cimento, Suppl.*, 6, 1063 (1957); R. A. Sack, *Mol. Phys.*, 1, 163 (1958).

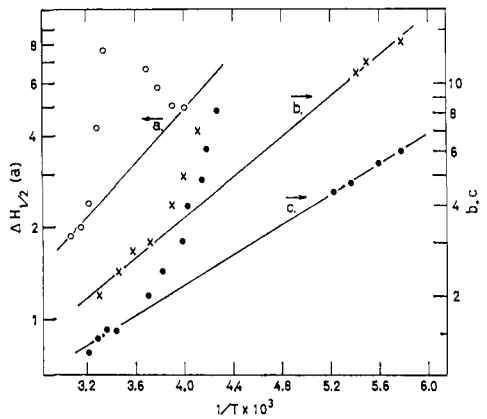

Figure 1. Temperature dependences of ln ($\Delta H_{1/2}$) of methyl signals in CD_2Cl_2 solutions: a (○), Fe(MePh(dtc))$_2$(tfd); b (×), Fe(Et$_2$(dtc))$_2$(tfd); c (●), Fe(Me$_2$(dtc))$_2$(tfd).

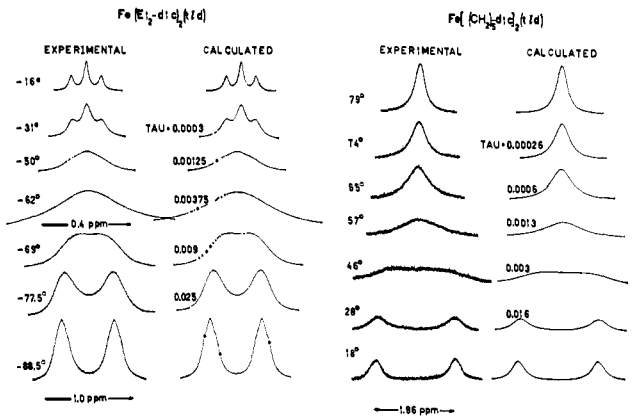

Figure 2. Experimental and calculated line shapes in CD_2Cl_2 solution: Fe(Et$_2$(dtc))$_2$(tfd), methyl signals, low-temperature process (inversion); Fe[(CH$_2$)$_5$(dtc)]$_2$(tfd), α-methylene signals, high-temperature process (C–N rotation).

compounds. The following values of $\Delta\nu$ (ppm) for methyl signals were found to be temperature independent in the slow-exchange regions of the indicated complexes: Fe(Me$_2$(dtc))$_2$(tfd), 0.430 (−98 to −80°); Fe(Et$_2$(dtc))$_2$(tfd), 0.605 (−98 to −85°); Fe(MePh(dtc))$_2$(tfd), 0.130 (−28 to −7°). These values were assumed constant in analysis of exchange-broadened spectra observed immediately above these temperature ranges.

Table III. Observed and Extrapolated Chemical Shift Separations between Methylene Protons in Two Fe(R$_1$R$_2$dtc)$_2$(tfd) Complexes in CD_2Cl_2 Solution

R$_1$,R$_2$ = Et		R$_1$,R$_2$ = (CH$_2$)$_5$	
Temp, °C	$\Delta\nu$,[a] ppm	Temp, °C	$\Delta\nu$,[b] ppm
92	1.95	79	1.72
83	1.95	72	1.75
76	1.94	64	1.78
71	1.93	57	1.80
67	1.93	52	1.81
53	1.83	46	1.82
47	1.79	40	1.83
41	1.75	28	1.85
35	1.74	19	1.86
29	1.72	10	1.87
25	1.70	0	1.88
20	1.68	−8	1.89
10	1.66	−18	1.90
−2	1.62		
−12	1.59		
−22	1.55		

[a] Values above 20° are extrapolated. [b] Values above 10° are extrapolated.

The line widths $\Delta H_{1/2}$ of the methylene resonances in Fe(Et$_2$(dtc))$_2$(tfd) and Fe[(CH$_2$)$_5$(dtc)]$_2$(tfd) were assumed to be independent of temperature between −20 and 90° because of identical values of 30.0 ± 0.5 Hz observed in the fast- and slow-exchange regions of both compounds. The methylene resonances are actually unresolved multiplets due to spin–spin coupling with other protons but are sufficiently relaxed due to the paramagnetism that they appear as single Lorentzian lines. These resonances were therefore treated as single lines in the simulation and good agreement with observed line shapes in the slow-exchange region was obtained. Shown in Figure 1 are plots of ln ($\Delta H_{1/2}$) *vs.* $1/T$ for methyl resonances of three complexes. The lines which connect the linear slow- and fast-exchange regions represent the values used in the line-shape analyses. Such a linear dependence is usually observed for paramagnetic systems[26] and implies viscosity control of line widths. For Fe(Et$_2$(dtc))$_2$(tfd), where signals due to environments A and B (low-temperature process) are represented by partially resolved methyl triplets (J = 7.1 Hz), the exchange problem was

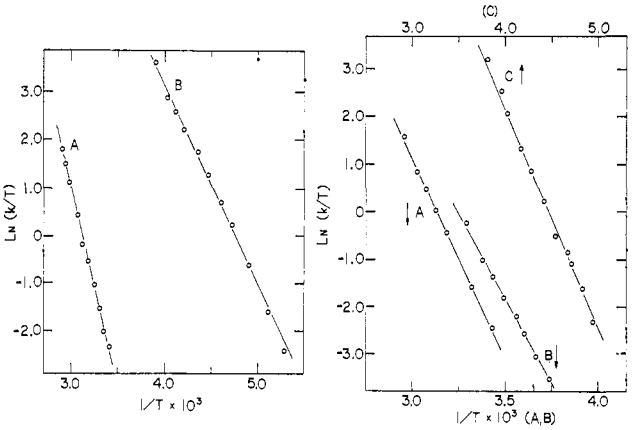

Figure 3. Kinetic plots for intramolecular processes of iron complexes in CD_2Cl_2 solution: left, high-temperature (A, C–N rotation) and low-temperature (B, inversion) processes of Fe(Et$_2$(dtc))$_2$(tfd); right, high-temperature process (C–N rotation) of Fe[(CH$_2$)$_5$(dtc)]$_2$(tfd) (A) and Fe(MePh(dtc))$_2$(tfd) (B), and low-temperature process (inversion) of Fe(Me$_2$(dtc))$_2$(tfd) (C).

treated as three two-site exchanges superimposed in one spectrum. The line widths for this compound are those for the individual components of each triplet and were determined in the slow-exchange region by trial-and-error fits to the broadened unresolved triplets. Examples of experimental calculated line shapes for low- and high-temperature processes are given in Figure 2.

The lifetime of a proton in environment A or B is defined as τ(sec), so the rate of exchange (sec^{-1}) between A and B is $1/\tau = k$. Activation parameters were determined by weighted least-squares fits to ln k *vs.* $1/T$ and ln (k/T) *vs.* $1/T$ plots for Arrhenius and Eyring parameters, respectively. The weighting of each k was determined experimentally by visually comparing calculated line shapes at various estimates of τ and assessing reasonable standard deviations. Eyring plots are shown in Figure 3 for all compounds studied. Points toward the centers of the lines were given greater weights in the least-squares fits. Final activation parameters are shown in Table IV along with appropriate error limits determined from assessed errors in individual rate constants, temperatures, and the standard deviation of the least-squares fit. Measurements were performed only at the concentrations listed; significant concentration variations were not possible due to limited solubilities. Line widths and chemical shifts were found to be somewhat dependent upon concentration and temperature. As shown in the text, these effects are not due to intermolecular exchange processes and appear to be inherent properties of the various systems.

Other Physical Measurements. Electronic spectra were obtained on a Cary Model 14 spectrometer. Magnetic moments in the solid and solution phases were determined by the Faraday (HgCo(NCS)$_4$ calibrant) and nmr methods, respectively. Infrared spectra were

(26) *Cf.*, *e.g.*, Z. Luz and S. Meiboom, *J. Chem. Phys.*, **40**, 2686 (1964).

Table IV. Kinetic Data for Dynamic Processes of $Fe(R_1R_2dtc)_2(tfd)$ in CD_2Cl_2 Solution

R_1, R_2	Process	$k^{298°}$, sec^{-1}	$\Delta F^{\ddagger}_{298°}$, kcal/mol	$\Delta H^{\ddagger}$, kcal/mol	$\Delta S^{\ddagger}$, eu	E_a, kcal/mol	Log A	Mol/g of solvent $\times 10^5$
Me, Me	Inversion[a,c]	$4.98 \pm 0.20 \times 10^4$	11.0 ± 1.5	9.2 ± 0.9	-6.1 ± 3.9	9.6 ± 0.9	11.8 ± 0.4	10.4
Et, Et	Inversion[a,c]	$1.02 \pm 0.10 \times 10^5$	10.6 ± 0.9	8.3 ± 0.6	-7.5 ± 2.7	8.8 ± 0.6	11.5 ± 0.2	11.1
Me, Ph	C–N rotation[b]	$1.29 \pm 0.10 \times 10^2$	14.9 ± 3.3	14.0 ± 2.1	-3.0 ± 7.8	14.6 ± 2.1	12.6 ± 0.6	9.14
Et, Et	C–N rotation[b]	$4.11 \pm 0.20 \times 10^1$	15.2 ± 1.8	16.4 ± 1.5	4.1 ± 4.5	17.1 ± 1.5	14.2 ± 0.3	14.1
$(CH_2)_5$	C–N rotation[b]	$4.38 \pm 0.20 \times 10^1$	15.2 ± 3.3	16.6 ± 2.4	4.7 ± 7.5	17.2 ± 2.4	14.3 ± 0.6	9.54

[a] Low-temperature process. [b] High-temperature process. [c] Lifetimes for inversion are possibly dependent on changes in thermal population of singlet and triplet spin states over the temperature range of measurement. While no departure from linearity is apparent in kinetic plots (Figure 3), this effect could introduce indeterminant errors in activation parameters.

measured on a Perkin-Elmer 337 spectrometer. Spectra of bromoform solutions were obtained on an expanded-scale recorder which permitted frequency measurements to ± 2-cm^{-1} accuracy.

Results and Discussion

Synthesis and Characterization. Complexes of the $Fe(R_1R_2dtc)_2(tfd)$ type are readily prepared by reaction 1, which proceeds smoothly in tetrahydrofuran solution under anaerobic conditions at ambient temperature. The products are deep red-brown solids which are readily soluble in nonpolar solvents to give red-brown solutions. The precursor iron(II) complexes have been used in most cases without isolation and definite identification. However, one such complex, $Fe(Et_2(dtc))_2$, has been reported earlier and its X-ray powder pattern found to indicate isomorphism with its dimeric copper(II) and zinc(II) analogs.[21] The complex may have the lateral dimer structure observed for antiferromagnetic bis(dithiolene)iron species.[27] Owing to extreme sensitivity to oxygen, an accurate magnetic moment has not yet been obtained.

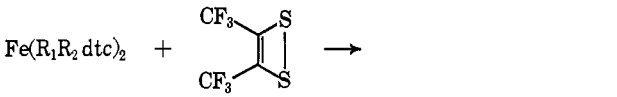

$$Fe(R_1R_2dtc)_2[S_2C_2(CF_3)_2] \quad (1)$$

Reaction 1 is, in effect, one of oxidative addition in which the iron is oxidized above the divalent state and the dithietene reduced below the α-dithione level upon complexation. As such it finds analogy with the reactions of metal carbonyls[27b,28] and the dithietene. The molecular structure of the prototype complex $Fe(Et_2(dtc))_2(tfd)$ has been established by the X-ray determination of Johnston, *et al.*,[29] and is depicted by **1**. Although the structure will be described in detail elsewhere,[29] certain of its features essential to the present study are noted here. The molecular configuration is roughly octahedral and therefore dissymmetric. The point-group symmetry is C_2, with the twofold axis passing through the iron and bisecting the C–C bond of the dithiolene ring. The nitrogen atoms possess a nearly coplanar arrangement of bonds, and the S_2C–N distances of 1.302 Å, comparable to those in other dithiocarbamate complexes,[2] clearly indicate appreciable double-bond character. Because the dithiocarbamate ligands are expected to retain the formal uninegative oxidation level upon reaction with the dithietene, the dimensions of the dithiolene ring are of prime importance in assessing electron redistribution upon product formation. The C–C (1.360 Å) and C–S

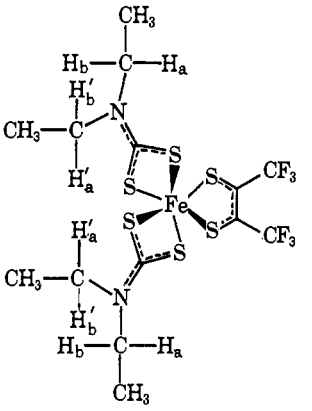

1

(1.702 Å) distances in this ring do not indicate reduction of the diethietene to the dithiolate level, as in $(Ph_3PCl)[Au(tfd)_2]$[30] (corresponding average values 1.31 and 1.76 Å). These distances are in reasonable agreement with those found in $[Ni(tfd)_2]\cdot$perylene[31] and are even closer to those in $[Ph_3AsFe(tfd)_2]$.[32] Because in these and other neutral bis(dithiolene) complexes the generally accepted electronic description[33] indicates an average oxidation level per ligand of $1-$, it is concluded that, in an approximate sense, one electron has been transferred from iron to $(CF_3)_2C_2S_2$ in $Fe(Et_2(dtc))_2(tfd)$ and analogous complexes. The average Fe–S (dithiocarbamate) distance of 2.310 Å compares favorably with that (2.317 Å) in the predominantly low-spin complex $Fe(S_2COEt)_3$.[16]

Similar reactions between $M(R_1R_2dtc)_2$ (M = Mn, Co) or $Ru(R_1R_2dtc)_2(CO)$ and the dithietene afford products analogous to those in the iron series. No X-ray structural data are as yet available for any of these complexes, but the similarity of their infrared spectra to those of their iron analogs strongly suggests equivalent structures. Their pmr spectra usually reflect a chiral structure and/or restricted C–N bond rotation, and thus convey the structural information contained in the spectra of the iron complexes, which are analyzed in detail below. The pmr spectrum of $Mn(Et_2(dtc))_2(tfd)$ at 30° gave very broad, featureless

(27) (a) J. F. Weiher, L. R. Melby,and R. E. Benson, *J. Amer. Chem. Soc.*, 86, 4329 (1964); (b) A. L. Balch, I. G. Dance, and R. H. Holm, *ibid.*, 90, 1139 (1968); (c) W. C. Hamilton and I. Bernal, *Inorg. Chem.*, 6, 2003 (1967).

(28) (a) A. Davison, N. Edelstein, R. H. Holm, and A. H. Maki, *ibid.*, 2, 1227 (1963); (b) *ibid.*, 3, 814 (1964); (c) *J. Amer. Chem. Soc.*, 86, 2799 (1964).

(29) D. L. Johnston, W. L. Rohrbaugh, and W. D. Horrocks, Jr., *Inorg. Chem.*, in press.

(30) J. H. Enemark and J. A. Ibers, *Inorg. Chem.*, 7, 2636 (1968).

(31) R. D. Schmitt, R. M. Wing, and A. H. Maki, *J. Amer. Chem. Soc.*, 91, 4394 (1969).

(32) E. F. Epstein, I. Bernal, and A. L. Balch, *Chem. Commun.*, 136 (1970); E. F. Epstein and I. Bernal, results to be published.

(33) G. N. Schrauzer, *Accounts Chem. Res.*, 2, 72 (1969).

signals and was not further investigated. Reactions involving $Ni(Et_2(dtc))_2$ and $Pd(Et_2(dtc))_2$ have given mixtures of products from which only $[Ni(tfd)_2]^-$ [28a] and $[Pd(tfd)_2]^-$ [28b] have thus far been identified. $Zn(Et_2(dtc))_2$ did not react under conditions which led to the formation of other $M(R_1R_2dtc)_2(tfd)$ complexes.

Although magnetic properties will be dealt with in a subsequent publication,[20] limited data are cited here to support the existence of a singlet–triplet spin equilibrium for $Fe(R_1R_2(dtc))_2(tfd)$ complexes. Magnetic moments in the crystalline and solution phases at ambient temperature are given in Table V. These values, while

Table V. Stretching Frequencies and Magnetic Data for $M(R_1R_2dtc)_2(tfd)$ and $M(R_1R_2dtc)_3$ Complexes

Complex	ν_{CN}, cm^{-1} [a]	μ_{eff}, BM: Solid (22°)	μ_{eff}, BM: CH_2Cl_2 [b] (30°)
$Fe(Me_2(dtc))_2(tfd)$	1533	1.01	1.13, 1.17[f]
$Fe(Et_2(dtc))_2(tfd)$	1507	2.25	1.34
$Fe(Me,CH_2Ph(dtc))_2(tfd)$	1508	1.75	1.20
$Fe(MePh(dtc))_2(tfd)$	1472	1.27	0.9
$Fe[(CH_2)_4(dtc)]_2(tfd)$	1501	1.13	1.50
$Fe[(CH_2)_5(dtc)]_2(tfd)$	1503	1.18	1.42
$Ru(Me_2(dtc))_2(tfd)$	1534	[c]	Dia
$Ru(Et_2(dtc))_2(tfd)$	1506	Dia	Dia
$Ru(MePh(dtc))_2(tfd)$	1473	[c]	Dia
$Co(Me_2(dtc))_2(tfd)$	1536	1.70	[c]
$Co(Et_2(dtc))_2(tfd)$	1508	1.79	[c]
$Mn(Et_2(dtc))_2(tfd)$	1511	4.00	[c]
$Fe(Et_2(dtc))_3$	1493	[d]	[d]
$Co(Et_2(dtc))_3$	1494	Dia	Dia
$Co(MePh(dtc))_3$	1467	Dia	Dia
$Ru(Et_2(dtc))_3$	1494	[e]	[c]

[a] Bromoform solution, ±2 cm^{-1}. [b] Solutions *ca.* 0.08 *M*, 5% v/v in TMS. [c] Not measured. [d] For magnetic data of $Fe(R_1R_2(dtc))_3$ complexes, *cf.* ref 3–5. [e] $S = 1/2$ (*cf.* ref 2). [f] Determined by the Gouy method.

usually quite small, are reproducible on different samples and are not due to contamination by small amounts of iron dithiolene[27b] and $Fe(R_1R_2dtc)_3$ [3–5] impurities, which would have been removed by the work-up procedure. In dichloromethane solution the moments of $Fe(Et_2(dtc))_2(tfd)$ range from 1.00 (−50°) to 1.40 BM (45°) and are reversible with temperature. All moments are within the limits $0 < \mu_{eff} < 2.8$ BM consistent with the spin equilibrium. The temperature dependence of the magnetic moment of crystalline $Fe(Et_2(dtc))_2(tfd)$ at 80–400°K also conforms to a thermal distribution over the two spin states.[20] Population of the triplet state is responsible for the isotropic shifts observed in the nmr spectra of the iron complexes.

Nmr Spectra of Iron Complexes. Proton and fluorine chemical shift data are set out in Table II. Spectra of the iron complexes are of greatest interest because of two properties. First, throughout the experimental temperature range of *ca.* −100 to 90° chemical shifts usually contain significant isotropic contributions due to fast averaging over singlet and triplet spin states. The magnitudes of the isotropic shifts, which are negative (downfield), may be estimated by comparison with those of the analogous diamagnetic ruthenium compounds. The pmr spectrum of a typical complex, $Fe[(CH_2)_5(dtc)]_2(tfd)$, is given in Figure 4. Second, the spectra of methylene and methyl protons reveal lineshape changes and coalescence phenomena which are

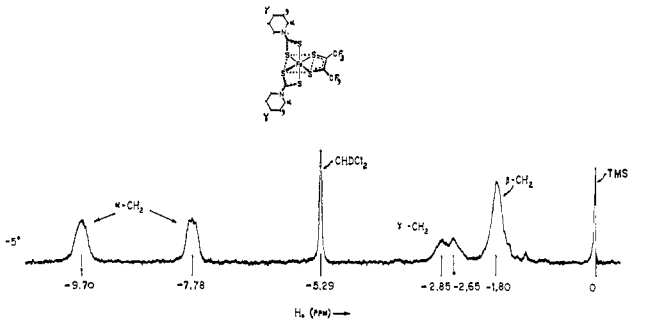

Figure 4. Pmr spectrum (100 MHz) of $Fe[(CH_2)_5(dtc)]_2(tfd)$ in CD_2Cl_2 solution at −5° illustrating the chemical shift separations due to isotropic interactions.

indicative of two types of environmental averaging processes. Chemical shift changes due to these processes are superimposed on the generally increasing negative chemical shifts with increasing temperature due to larger thermal populations of the triplet state.

Evidence cited below indicates that the two averaging processes are intramolecular in origin. Stereochemical rearrangements consistent with the static structure **1**, the essential features of which are assumed for all other iron complexes, are inversion of the molecular configuration ($\Lambda \rightleftharpoons \Delta$) and rotation about the C–N bonds. The latter process has been detected in the pmr spectra of certain dithiocarbamate[34,35] and thiuram disulfide[36] complexes and dithiocarbamate esters.[37] Detailed kinetic analysis has been reported only for the esters. The pmr spectrum of $Fe[(CH_2)_5(dtc)]_2(tfd)$ in CD_2Cl_2 under slow exchange conditions (−92°) reveals four α-methylene signals with a total spread of 3.87 ppm (Table II). Under similar conditions the spectrum of $Fe(Et_2(dtc))_2(tfd)$ contains three methylene signals with intensities 1:1:2 from low (−7.05 ppm) to high field (−4.40 ppm), and two equally intense methyl signals separated by 0.61 ppm. The methylene signal multiplicities are consistent with a static configuration of type **1**, in which four protons (H_a, H_a', H_b, H_b' in **1**) are magnetically nonequivalent because of slow inversion *and* bond rotation. As the temperature is increased pairs of methylene signals of each complex undergo broadening and coalescence (low-temperature process) until two well-defined resonances of equal intensity appear below *ca.* −10°. These spectral changes are consistent with either inversion or bond rotation, since either process averages two previously inequivalent pairs of methylene protons. (With reference to structure **1**, inversion will average H_a with H_b and H_a' with H_b', while bond rotation will average pairs of protons, each member of which is on a different carbon.) Similar comments apply to the methyl spectra of $Fe(Et_2(dtc))_2(tfd)$ (*cf.* Figure 2) and $Fe(Me_2(dtc))_2(tfd)$, in which two resonances are averaged by the low-temperature process.[38] At still higher temperatures the methylene

(34) B. F. G. Johnson and K. H. Al-Obaidi *Chem. Commun.*, 876 (1968); B. F. G. Johnson, K. H. Al-Obaidi, and J. A. McCleverty, *J. Chem. Soc. A*, 1668 (1969).
(35) D. C. Pantaleo and R. C. Johnson, *Inorg. Chem.*, **9**, 1248 (1970).
(36) H. C. Brinkhoff, A. M. Grotens, and J. J. Steggerda, *Recl. Trav. Chim. Pays-Bas*, **89**, 11 (1970).
(37) C. E. Holloway and C. H. Gitlitz, *Can. J. Chem.*, **45**, 2659 (1967).
(38) These complexes are of the general formulation $M(A–A)_2(B–B)$. If C–N bond rotation is slow, the averaging of methyl signals due to inversion will depend on the mechanism of this process. The considerations of Fortman and Sievers[39] applied to such species show that in-

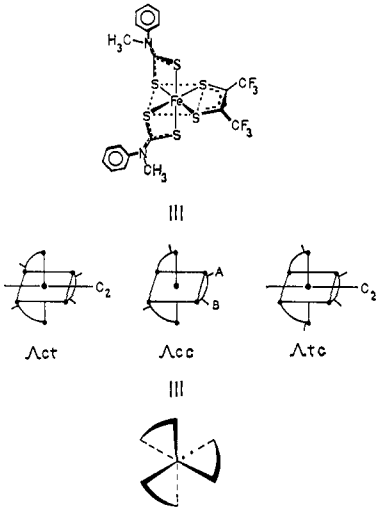

Figure 5. The cis,cis (cc) and simplified representations of the cc, cis,trans (ct), and trans,cis (tc) isomers of Fe(MePh(dtc))$_2$(tfd), all shown in the Λ absolute configuration.

signals of Fe[$(CH_2)_5$(dtc)]$_2$(tfd) (*cf.* Figure 3) and Fe(Et_2-(dtc))$_2$(tfd) broaden and coalesce to a single feature at temperatures below *ca.* 80° (high-temperature process).

The intramolecular nature of the processes just described is indicated by results of experiments of the following type. Solutions of Fe(Me_2(dtc))$_2$(tfd) and Fe(Et_2(dtc))$_2$(tfd) establish equilibrium 2 upon mixing at ~25°. Pmr spectra reveal separate sets of signals due to

$$\text{Fe}(Me_2(\text{dtc}))_2(\text{tfd}) + \text{Fe}(Et_2(\text{dtc}))_2(\text{tfd}) \rightleftharpoons 2\text{Fe}(Me_2(\text{dtc}))(Et_2(\text{dtc}))(\text{tfd}) \quad (2)$$

each species. The methylene resonances of the ethyl and methylethyl complexes separately coalesce with increasing temperature, and no evidence of dynamic ligand exchange was found up to 90°. Rates of intramolecular rearrangements are therefore much faster than rates of ligand exchange on the pmr time scale.

Because the spectral changes associated with the low- and high-temperature processes of the aforementioned complexes do not necessarily identify either process as inversion or bond rotation, attention is directed to the properties of the related but unsymmetrically substituted species Fe(MePh(dtc))$_2$(tfd). Three geometrical isomers are possible for this complex in the limit of slow C–N bond rotation: cis,trans (ct), cis,cis (cc), and trans,cis (tc). These are depicted in Figure 5 and are designated according to the orientation of the flagged (Ph or Me) and unflagged (Me or Ph) "ends" of the two dithiocarbamate chelate rings. Each isomer is enantiomeric and can exist in the Δ,Λ absolute configurations. The ct and tc isomers possess a twofold symmetry axis, whereas the cc form has no symmetry. Consequently, in the latter the two methyl and trifluoromethyl (A,B) groups are inequivalent. The ^{19}F and pmr spectra of Fe(MePh(dtc))$_2$(tfd) in a temperature interval encompassing the low- and high-temperature processes are shown in Figures 6 and 7, respectively. These spectra serve to identify the two processes and provide sufficient constraints upon the low-temperature process that its mechanism may be deduced with considerable certainty.

version does not necessarily average the environments of A–A ring substituents.

(39) J. J. Fortman and R. E. Sievers, *Inorg. Chem.*, 6, 2022 (1967).

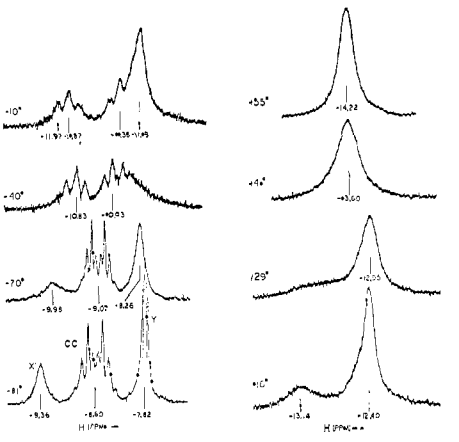

Figure 6. Temperature dependence of the ^{19}F spectrum of Fe(MePh(dtc))$_2$(tfd) in CD_2Cl_2 solution. Signals x, y refer to the ct, tc isomers; cc = cis,cis isomer. Sweep widths are not the same at each temperature.

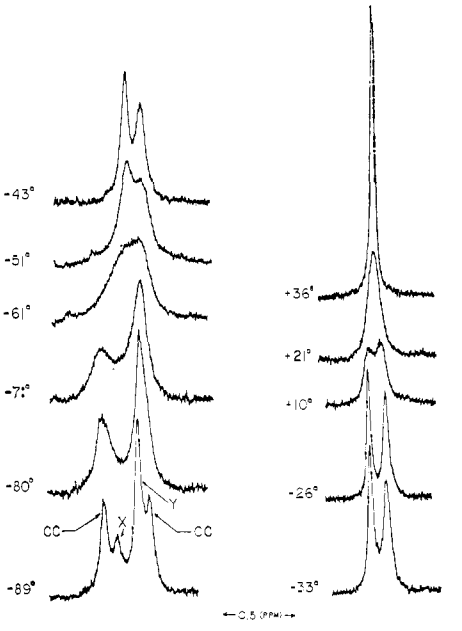

Figure 7. Temperature dependence of the pmr spectrum of Fe(MePh(dtc))$_2$(tfd) in CD_2Cl_2 solution. Signals x, y refer to the ct, tc isomers; cc = cis,cis. The vertical alignment of spectra does not imply a fixed chemical shift scale; signals move progressively to lower field as the temperature is increased.

The fluorine spectra under slow-exchange conditions (−81°) show two singlets at −8.31 and −9.96 ppm with intensity ratio 2.4:1 (signals y and x). These features must arise from the ct and tc forms; neither feature can be assigned to a specific isomer. The multiplet centered at −9.14 ppm arises from the A_3B_3 spin system of the cc isomer. The intensity ratio cc/(ct + tc) is 0.85. The most significant information conveyed by these spectra is that the signals of the ct and tc forms average with each other by a mechanism which does not involve the cc isomer. At −10° these signals have coalesced to a single feature at −11.89 ppm. The ratio cc/(ct + tc) is 1.0 at this temperature. The pmr spectra also reveal the ct ⇌ tc interconversion and further show that the cc isomer is undergoing rearrangement in the same temperature interval. Four methyl signals are well resolved at −89° with the intensity relations y/x = 2.6

and cc/(ct + tc) = 0.90, in good agreement with the ^{19}F results. As the temperature is increased these signals undergo exchange broadening followed by emergence of two sharp resonances which are maintained up to *ca.* $-10°$. At $-10°$ cc/(ct + tc) = 1.1 or 0.91, depending upon the assignment. Either of these intensity ratios is consistent with the separate averaging of signals x and y and the two cc signals, and with no other averaging scheme. This result is of course compatible with the fluorine spectra and is of prime importance because it demonstrates that the cc isomer is also involved in a low-temperature rearrangement process which equilibrates the two different methyl environments. The pmr spectrum of $Fe(Me,CH_2Ph(dtc))_2(tfd)$ in CD_2Cl_2 undergoes similar changes in the -90 to $-10°$ range. Four methyl signals at the low-temperature end of the range are averaged to two signals above *ca.* $-20°$.

The nmr results impose the following constraints on the mechanism of the low-temperature process of $Fe(MePh(dtc))_2(tfd)$. (i) The ct $\rightleftharpoons$ tc interconversion must proceed by a path which does not involve the cc isomer. (ii) The rearrangement reaction of the cc isomer must average the methyl environments while simultaneously *not* averaging the trifluoromethyl environments. These two constraints cannot be reconciled with a rearrangement process which involves C–N bond rotation only. Consequently, the processes responsible for the proton and fluorine spectral changes below *ca.* 0° must be metal-centered rearrangements. Because the three geometrical isomers differ only in the orientation of N substituents well removed from the $Fe–S_6$ core, an additional constraint, which is physically reasonable but not necessarily required by the spectral results, is added. (iii) The same type of mechanism must apply to the processes in i and ii.

Mechanism of the Low-Temperature Processes of $Fe(MePh(dtc))_2(tfd)$. The mechanistic considerations pertinent to metal-centered rearrangements of this complex are similar to those given in detail for the isomerization and racemization reactions of trischelates of the type $M(A–A')_3$,[40] in which A–A′ is an unsymmetrically substituted ligand with otherwise identical donor atoms. $Fe(MePh(dtc))_2(tfd)$ is of the type $M(A–A')_2(B–B)$ and may be treated in an analogous fashion. Rearrangement reactions can proceed by a bond-rupture mechanism involving a five-coordinate transition state with an idealized trigonal-bipyramidal (TBP) or square-pyramidal (SP) geometry and dangling axial or equatorial (basal) ligands. A second type of reaction pathway involves no metal–ligand bond rupture and idealized trigonal-prismatic (TP) transition states which are produced by means of various twist motions of the chelate rings about artificial threefold axis bisecting opposite octahedral faces.[40,41] In order to establish the mechanism of the low-temperature process, each pathway must be carefully examined. Because of the generality of the mechanistic arguments for the $M(A–A')_2(B–B)$ case, which has not previously been treated,[42] transition states and possible isomeric interconversions are described in detail for the various mechanisms. A dissociative mechanism requiring rupture of two metal–ligand bonds is discounted because of presumably unfavorable activation energies.

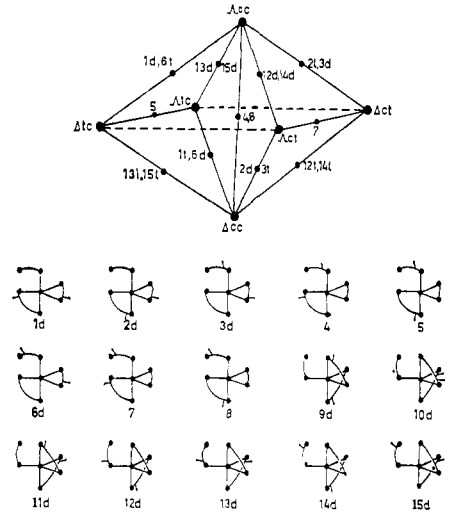

Figure 8. Topological correlation diagram for the interconversion of $M(A–A')_2(B–B)$ isomers through TBP transition states. The *d* and achiral transition states produced by rupture of inequivalent bonds in the ct, tc, and cc isomers[43] are shown.

Bond-rupture mechanisms are considered first. All possible TBP transition states may be obtained by rupture of the inequivalent metal–ligand bonds in Δ,Λ_{ct}; Δ,Λ_{tc}; and Δ,Λ_{cc}.[43] These number 26 and include 11 enantiomeric (*dl*) pairs and four which are achiral. Transition states are illustrated in Figure 8. Three pairs (9*dl*, 10*dl*, 11*dl*) are nonfunctional with respect to inversion and isomerization of the parent isomer and four other transition states (4, 5, 7, 8) are similarly inactive in geometrical isomerization. Also given in Figure 8 is a topological correlation diagram[44] which summarizes the possible interconversions of isomers proceeding through TBP transition states produced by bond rupture. The diagram takes the form of an octahedron with two opposite edges missing and two apices joined by a diagonal. Isomers are located at the apices and transition states at the midpoint of edges and the diagonal. The type of interconversion represented in the diagram is illustrated by the rupture of bond c of Λ_{ct} shown in Figure 9. The most significant features of the correlation diagram are that the ct $\rightleftharpoons$ tc interconversion can take place only through a cc intermediate, and that the cc isomer can invert by a direct process. The first feature violates constraint i and the second violates constraint ii, because inversion of cc through transition states 4 and 8 results in averaging of environments of the trifluoromethyl groups, A and B. Therefore, a mechanism in which TBP transition states produced by bond rupture pass directly to products is eliminated.

The TBP mechanism has been further investigated by allowing each transition state arising from bond rupture[43] to undergo pseudorotation[45] (pr) once about each

(40) J. G. Gordon, II, and R. H. Holm, *J. Amer. Chem. Soc.*, 92, 5319 (1970).
(41) C. S. Springer, Jr., and R. E. Sievers, *Inorg. Chem.*, 6, 852 (1967).
(42) The twist mechanism for the related $M(A–A')_2X_2$ case has been described elsewhere: N. Serpone and R. C. Fay, *ibid.*, 6, 1835 (1967).

(43) The following transition states result from rupture of the indicated bonds (*cf.* Figure 9) of the Λ isomers. Λ_{ct}: a, 10*d* + 2*d*; b, 14*d* + 7; c, 12*d* + 3*l*; Λ_{tc}: a, 9*d* + 1*l*; b, 13*d* + 5; c, 15*d* + 6*d*; Λ_{cc}: a, 11*d* + 1*d*; b, 11*d* + 2*l*; c, 15*d* + 8; d, 12*d* + 4; e, 14*d* + 6*l*; f, 13*d* + 3*d*. Designation of configurations as *d* and *l* is arbitrary and follows the convention used earlier.[40]
(44) E. L. Muetterties, *J. Amer. Chem. Soc.*, 90, 5097 (1968).
(45) F. H. Westheimer, *Accounts Chem. Res.*, 1, 70 (1968).

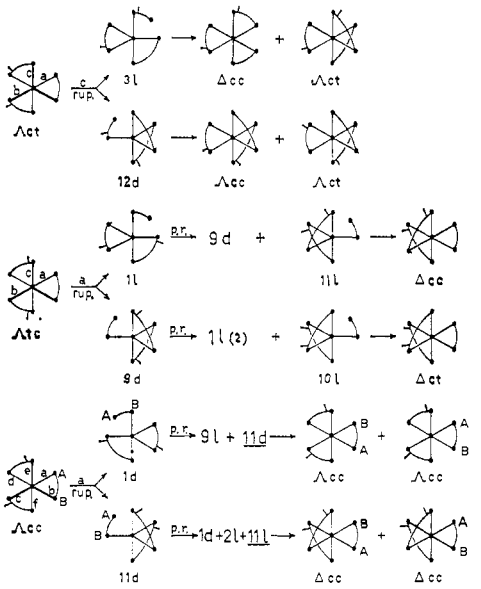

Figure 9. Illustrative rearrangement pathways of M(A–A′)$_2$(B–B) *via* TBP transition states: top, transition states and products from rupture of bond c of Λ_{ct}; center, transition states from rupture of bond a of Λ_{ct}, transition states obtained by pseudorotation (pr) of 1*l* and 9*d*, and products from 11*l* and 10*l*; bottom, transition states from rupture of bond a of Λ_{cc}, transition states obtained by pseudorotation of 1*d* and 11*d*, and products from 11*d* and 11*l*. A and B refer to CF_3 groups.

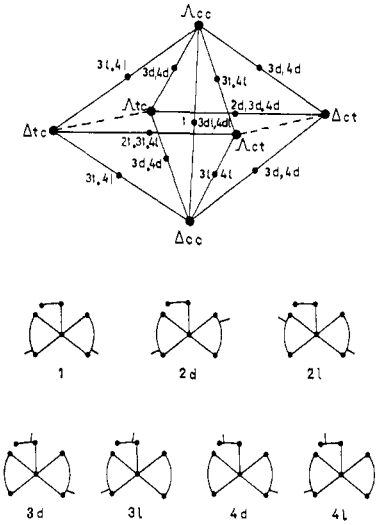

Figure 10. Topological correlation diagram for the interconversion of M(A–A′)$_2$(B–B) isomers through SP-axial transition states (primary process). The seven transition states produced by rupture of inequivalent bonds in the ct, tc, and cc isomers[46] are shown.

of its three equatorial metal–ligand bonds. Although the details are too lengthy to reproduce here, it is readily shown that only the sequences of eq 3 or their mirror images lead to direct ct $\rightleftharpoons$ tc interconversion. The second sequence is illustrated in Figure 9. This

$$\Lambda_{ct} \xrightarrow[\text{rupture}]{a} 10d \xrightarrow{pr} 9l \longrightarrow \Delta_{tc}$$
$$\Lambda_{tc} \xrightarrow[\text{rupture}]{a} 9d \xrightarrow{pr} 10l \longrightarrow \Delta_{ct} \qquad (3)$$

type of rearrangement path may be eliminated at once if it is assumed that all initial transition states from ct and tc pseudorotate with equal probability about their

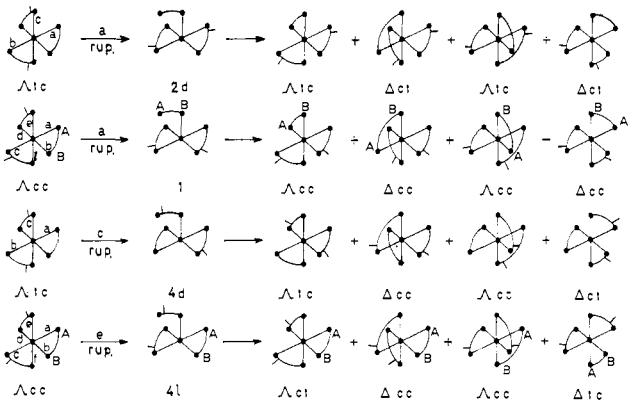

Figure 11. Illustrative rearrangement pathways of M(A–A′)$_2$(B–B) *via* SP-axial transition states and the primary process. Analogous processes are shown for Λ_{tc} and Δ_{cc}. A and B refer to the CF_3 groups.

three axes. In such a case the cc, ct, and tc isomers would be interconverted in the low-temperature process, contrary to observation. However, the TBP-pseudorotation pathway may be discounted in more specific terms by the imposition of constraint iii. Bond-a rupture in the above sequences corresponds to breaking of bond a (or b) in the cc isomer. As shown in Figure 9, rupture of bond a in Λ_{cc} leads to 1*d* and 11*d*, which generate 11*d* and 11*l*, respectively, by pseudorotation. The former produces Λ_{cc} and the latter Δ_{cc}, but only with equilibration of the environments of trifluoromethyl groups in each case. Because this is not observed, the TBP-pseudorotation bond-rupture pathway is not an acceptable mechanism.

SP transition states obtained from rupture of inequivalent bonds in Δ,Λ_{ct}; Δ,Λ_{tc}; and Δ,Λ_{cc} are given in Figure 10 and consist of three enantiomeric pairs and one symmetrical form.[46] All contain the dangling ligand in the axial position. SP-basal transition states are kinetically equivalent to those of the TBP-equatorial type,[40] which have been eliminated as possible transition states. Rearrangement *via* an SP-axial mechanism is complicated by the possibility of two microscopically reversible pathways for the formation of transition states and products. These pathways, designated as primary (p) and secondary (s), have been described elsewhere.[40] Attention is directed to the p process, which on an *a priori* basis is much more likely than the s process because of the lesser degree of ligand motion required in forming products. Shown in Figure 10 is the correlation diagram for the p process, examples of which are provided in Figure 11. Unlike the TBP case, the SP mechanism allows direct interconversion of ct and tc isomers but does not permit inversion without isomerization. Thus, the process $\Lambda_{tc} \rightleftharpoons \Delta_{ct}$, for example, can occur through transition states 2*d*, 3*d*, and 4*d*. Of the three only 2*d* does not generate the cc form if attack of the dangling end at each of the four basal positions is of comparable probability. This reaction path may be eliminated by constraint iii. As shown in Figure 11, rupture of the analogous bond in Λ_{cc} leads to racemization and averaging of the trifluoromethyl A,B environments. Reactions *via* 3*d* and 4*d* are highly im-

(46) The following transition states result from rupture of the indicated bonds (*cf.* Figure 9) of the Λ isomers. Λ_{ct}: a, 2*l*; b, 4*l*; c, 3*l*; Λ_{tc}: a, 2*d*; b, 3*d*; c, 4*d*; Λ_{cc}: a and b, 1; c, 4*d*; d, 3*l*; e, 4*l*; f, 3*d*.

probable because each transition state could produce only the ct (tc) isomer by attack at just one basal position. More specifically, such attack would require, in effect, implausible discrimination between two sulfur atoms of a dithiocarbamate ligand by the attacking end, as illustrated for Λ_{tc} and Λ_{cc} in Figure 11. On these grounds the SP-primary mechanism is eliminated. Consideration of mixtures of p and s mechanisms is more involved, but leads to the conclusion that no pathway for the tc $\rightleftharpoons$ ct interconversion and rearrangement of cc exists which satisfies the three constraints and does not require formation of product so selective as to be physically unrealistic.

The remaining reaction pathway to be considered involves the twist mechanism. The idealized TP transition states may be generated by twist motions about axes which are designated as pseudo (p) and imaginary (i) C_3 axes when the notation of Springer and Sievers[41] is applied to the $M(A-A')_2(B-B)$ case. The Λ_{ct} and Λ_{cc} isomers viewed down their p-C_3 and one of their i-C_3 axes are shown in Figure 12. Twists about these axes produce the indicated transition states. The remaining transition states may be generated by twists about the pseudo and imaginary C_3 axes of Δ,Λ_{ct}; Δ,Λ_{tc}; and Δ,Λ_{cc} isomers.[47] A total of ten transition states is obtained, which include four enantiomeric pairs. The possible interconversions, all of which proceed with inversion, are summarized by the correlation diagram in Figure 12. The direct ct $\rightleftharpoons$ tc interconversion is allowed and is illustrated for $\Lambda_{ct} \rightarrow \Delta_{tc}$ in this figure. In order to assess this twist pathway constraint iii is imposed and inversion of Λ_{cc} by twists about the corresponding axes is examined. This process is set out in Figure 12. A,B and a,b are the two trifluoromethyl and methyl groups, respectively. Inversion effected by twist about i-C_3' and passage through transition state 6 averages the environments of the two trifluoromethyl and methyl groups, and thus violates constraint ii. However, twist about p-C_3 and passage through transition state 5 preserves the magnetic inequivalence of the trifluoromethyl groups while averaging the environments of the methyl groups. Of all pathways considered, only the p-C_3 twist conforms to constraint ii while simultaneously satisfying constraint i. Consequently, *the primary low-temperature process of the ct, tc, and cc isomers of Fe(MePh(dtc))$_2$(tfd) is identified as inversion of configuration proceeding by a twist motion (or its operational equivalent) about the p-C_3 axes.*[48]

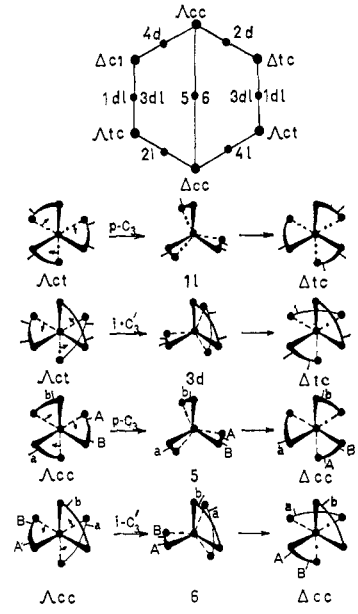

Figure 12. Topological correlation diagram for the interconversion of $M(A-A')_2(B-B)$ isomers by a twist mechanism. Twist motions about the p-C_3 and one of the imaginary C_3 axes of Λ_{ct} and Λ_{cc} are illustrated. A,B and a,b refer to the CF_3 and CH_3 groups, respectively.

High-Temperature Process of Fe(MePh(dtc))$_2$(tfd). Nmr spectral changes above 0° are illustrated in Figures 6 and 7. The fluorine spectra result from averaging of the coalesced ct–tc signal with the two resonances of the cc isomer. Similar behavior is seen in the pmr spectra. The two methyl signals coalesce at *ca.* 13°, and at higher temperatures a single sharp resonance is observed. These changes are consistent with passage from slow to rapid C–N bond rotation with increasing temperature. If the p-C_3 twist is the only metal-centered rearrangement operative in this region, the high-temperature process may be assigned to C–N bond rotation. The pmr spectra were subjected to a full line-shape analysis and kinetic parameters for C–N rotation are given in Table IV.

Low- and High-Temperature Processes of Other Iron Complexes. As stated above, the spectral changes of other Fe(R_1R_2dtc)$_2$(tfd) complexes in the low- and high-temperature regions do not unambiguously identify the rearrangement process occurring in each region. The data in Table VI permit comparison of preexchange

Table VI. Preexchange Lifetimes at ^{19}F Coalescence Temperatures of Fe(MePh(dtc))$_2$(tfd) for Other Fe(R_1R_2dtc)$_2$(tfd) Complexes in CD_2Cl_2 Solution

R_1, R_2	Spectrum	$\tau_{inversion}$ (−50°), sec	$\tau_{CN\ rotation}$ (28°), sec
Me, Ph	^{19}F	0.0040[a]	0.011[a]
	^{1}H		0.010
$(CH_2)_5$[b]	^{1}H		0.016
Et, Et[b]	^{1}H	0.0013	0.015
Me, Me[b]	^{1}H	0.0055	

[a] Estimated by approximate computer fit to experimental coalescence spectra. [b] Lifetimes calculated at indicated temperatures by total line-shape analysis.

(47) The following transition states result from twists about the indicated axes of the Λ isomers: Λ_{ct}: p-C_3, 1*l*; i-C_3, 4*l*(2); i-C_3', 3*d*; Λ_{tc}: p-C_3, 1*l*; i-C_3, 2*l*(2); i-C_3', 3*l*; Λ_{cc}: p-C_3, 5; i-C_3, 2*d*; i-C_3', 6; i-C_3'', 4*d*. Axes are defined in an analogous manner for the three isomers. Note that two of the imaginary axes of ct and tc are equivalent. Transition states 1*l*, 3*d*, 5, and 6 are illustrated in Figure 12 and the remainder may be deduced from the correlation diagram in this figure.

(48) One of the referees has suggested a transition state for the low-temperature process which is different from those considered above. The complex such as **1** is regarded as containing two uninegative dithiocarbamate ligands and an iron(II)–α-dithione unit which then undergoes an intramolecular two-electron redox reaction producing a coordinated thiuram disulfide molecule and an iron(II)–dithiolate unit. Rotational motions about the resultant disulfide bond, with or without formal Fe–S bond rupture, can be envisaged which produce inversion of cc and interconversion of ct and tc with inversion and conform to constraints i and ii. Such a pathway cannot be eliminated by the available nmr evidence, but is considered less likely than the twist mechanism. The electronic description of the static form of the complex is not consistent with the X-ray structural evidence summarized above. Considerable electronic rearrangement is required together with nuclear motions of the two *cis*-dithiocarbamate sulfurs, which are separated by 3.56 Å in **1**. Further, it is not clear why a redox process of this sort would be subject to mild thermal excitation, *i.e.*, why, in this context, the stable isolable forms of the complexes would not contain coordinated thiuram disulfide instead of two dithiocarbamate groups.

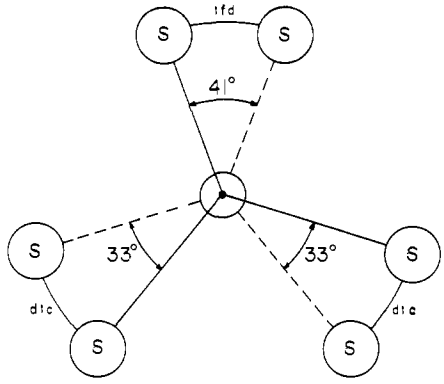

Figure 13. Structure of $Fe(Et_2(dtc))_2(tfd)$ viewed down the p-C_3 axis illustrating the twist angles between the upper and lower S_3 triangles.

lifetimes for inversion and bond rotation of Fe(MePh-(dtc))$_2$(tfd), determined at ^{19}F coalescence temperatures, with lifetimes for processes of related complexes. The similarity of values provides good evidence that the low- and high-temperature processes are inversion and bond rotation, respectively. A similar conclusion is reached from a comparison of activation parameters for high- and low-temperature processes (*cf.* Table IV) obtained by a total line-shape analysis. Values of $\Delta F^{\ddagger}$ are meaningful for such a comparison[49] and differ by less than 0.5 kcal/mol for each process. Free energies of activation for bond rotation also agree well with $\Delta F^{\ddagger}_{298°}$ = 15.1 kcal/mol for the related process of $Me_2NCSSEt$ in *n*-hexane,[50] although such close agreement is not necessarily expected. Assignment of low- and high-temperature processes of all iron complexes thus far studied to inversion and C–N bond rotation, respectively, is the reverse of that offered earlier for the R_1, R_2 = Me, Et, and $(CH_2)_5$ species,[18] at which time spectral data and demonstration of the twist mechanism for Fe(MePh(dtc))$_2$(tfd) were not available.

Physical Basis of Twist Mechanism. Analysis of the nmr spectra of Fe(MePh(dtc))$_2$(tfd) has provided the best available proof for the operation of a twist mechanism in the rearrangement reactions of trischelates. Motions of rings about real or p-C_3 axes have been described as Bailar or trigonal twists.[51] Twists about these or imaginary axes have been shown either not to be operative or not to be the only pathway consistent with kinetic data for inversion and geometrical isomerization of trischelates.[40,51b,52] The most detailed data are available for tris(β-diketonato)cobalt(III) complexes, the structural and electronic properties of which are consistent with an octahedral CoO_6 core.[53] Analysis of rate constants and activation parameters for inversion and isomerization of these complexes satisfactorily establishes that both processes take place predominantly or exclusively by bond rupture.[40,62a] The structure of $Fe(Et_2(dtc))_2(tfd)$ reveals an important feature which provides a plausible physical basis for operation of a twist mechanism in this and analogous complexes. A view of the structure down the p-C_3 axis, shown in Figure 13, reveals that the molecule is significantly distorted toward a trigonal-prismatic configuration. The upper and lower S_3 planes are roughly parallel with extremes of S···S approach, calculated from atomic coordinates,[29] being 2.53 and 2.80 Å. Other pairs of S_3 planes have approach distances of 1.75 to 3.05 Å. Their lack of even approximate parallelism severely diminishes the physical significance of rotation about an imaginary C_3 axis. The twist angles given in the figure specify the departure from an effective trigonal-prismatic geometry. Twice these values (66 and 82°) describes the extent of ring motion required for inversion and is to be contrasted with the 120° displacement necessary for a twist pathway in tris(diketonato) complexes.[54]

Pmr Spectra of Other Complexes. Chemical shift data are given in Table II. The lack of isotropic shifts in $Ru(R_1R_2dtc)_2(tfd)$ complexes and the consequent small chemical shift separations have prevented an examination of rearrangement reactions. Two methyl signals and two overlapping methylene triplets are observable in the spectra of the MePh and Et_2 complexes, respectively, near room temperature. At lower temperature only a slight broadening of these resonances was found. $Ru(Me_2(dtc))_2(tfd)$ exhibited only one methyl signal down to −85°. Large chemical shift differences were found in the spectra of $Co(Me_2(dtc))_2(tfd)$ and $Co(Et_2(dtc))_2(tfd)$. The three methylene signals of the latter at 30° imply slow inversion and bond rotation. Because of the very large line widths of these spin-doublet species, studies over a temperature range were not performed.

Infrared Spectra. A characteristic feature of dtc complexes is the C···N stretching absorption usually found in the range 1460–1550 cm^{-1}.[2,58] The values of ν_{CN} for $M(R_1R_2dtc)_2(tfd)$ complexes, given in Table V, reveal the same basic behavior previously observed for bis- and tris(dtc) chelates.[58a] Stretching frequencies are essentially independent of M at constant R_1 and R_2, decrease when R_1 and R_2 are larger than methyl, and decrease when R_1 or R_2 is an aryl group. The experimental uncertainties in activation parameters for bond rotation (Table IV) mask any relationship between these

(49) G. Binsch, *Top. Stereochem.*, 3, 97 (1968).

(50) In addition to $\Delta F^{\ddagger}$ the following activation parameters were obtained using the data of Gitlitz and Holloway:[37] $\Delta H^{\ddagger}$ = 11.7 kcal/mol, $\Delta S^{\ddagger}$ = −11.4 eu, E_a = 12.2 kcal/mol, log A = 10.7.

(51) (a) J. C. Bailar, Jr., *J. Inorg. Nucl. Chem.*, 8, 165 (1958); (b) R. C. Fay and T. S. Piper, *Inorg. Chem.*, 3, 348 (1964).

(52) (a) A. Y. Girgis and R. C. Fay, *J. Amer. Chem. Soc.*, 92, 7061 (1970); (b) J. R. Hutchison, J. G. Gordon, II, and R. H. Holm, *Inorg. Chem.*, in press.

(53) J. P. Fackler, Jr., *Progr. Inorg. Chem.*, 7, 361 (1966).

(54) Twist angles of less than 60° have been established for other Fe–S_6 species, *viz.*, Fe(*n*-Bu_2(dtc))$_3$[15] (32°) and $Fe(S_2COEt)_3$[18] (41°). The failure to detect more than one methyl signal down to −30° in the isotropically shifted pmr spectrum of Fe(MePh(dtc))$_3$[14] is apparently due to smaller inversion and rotation barriers than found for Fe(MePh-(dtc))$_2$(tfd). However, it is observed that in certain other cases significant distortions from an octahedral structure do not necessarily imply a low barrier to inversion or operation of a twist mechanism. Twist angles for $Co(S_2COEt)_3$[55a] and $Co(Et_2(dtc))_3$[55b] calculated from X-ray data are 43 and 44°, respectively. Related complexes exhibit the configurational stability generally observed for cobalt(III) species. Co-(S_2CO-*l*-menthyl)$_3$ has been separated into its $\Delta(lll)$, $\Lambda(lll)$ diastereoisomers,[56] and $[Co(S_2COCH_2CH_2SO_3)_3]^{3-}$ has been resolved and its racemization kinetics measured in aqueous solution.[57] For the latter, log A = 14.5 sec^{-1}, which is close to the values 14.7–16.4 obtained for the inversion and isomerization of tris(β-diketonates)[40,51b,52a] and less than those found in this work. It has been speculated elsewhere that low frequency factors and negative $\Delta S^{\ddagger}$ values (*cf.* Table IV) will be associated with twist processes.[51b,52a]

(55) (a) S. Merlino, *Acta Crystallogr., Sect. B*, 25, 2270 (1969); (b) S. Merlino, *ibid., Sect. B*, 24, 1441 (1968).

(56) H. Krebs and W. Schumacher, *Z. Anorg. Allg. Chem.*, 344, 187 (1966).

(57) H. Krebs, J. Diewald, H. Arlitt, and J. A. Wagner, *ibid.*, 287, 98 (1956).

(58) (a) J. Chatt, L. A. Duncanson, and L. M. Venanzi, *Suom. Kemistilehti B*, 29, 75 (1956); (b) F. A. Cotton and J. A. McCleverty, *Inorg. Chem.*, 3, 1398 (1964).

parameters and ν_{CN}. Data tabulated elsewhere[2] reveal no widespread correlation between C–N distances and ν_{CN}.

Finally, it is pointed out that the isotropic interactions responsible for the resolution in the nmr spectra of $Fe(R_1R_2dtc)_2(tfd)$ complexes are believed to be mainly dipolar in origin. Approximate calculations of the relevant geometric factors based on the known structure **1**[29] reveal that these factors should produce significant chemical shift differences among methylene protons of a given dtc ligand. Related conclusions have been reached by LaMar[59] for $Co(acac)_2(phen)$ species. An analysis of the isotropic shifts will be attempted upon completion of single-crystal paramagnetic resonance and magnetic susceptibility measurements of **1**.

Acknowledgment. This research was supported by the National Science Foundation under Grant No. GP-7576X. We thank Dr. D. Coucouvanis for a copy of ref 2 prior to publication, Drs. W. D. Horrocks, R. C. Fay, and I. Bernal for disclosure of unpublished results, and J. G. Gordon, II, and Dr. J. R. Hutchison for useful discussions.

(59) G. N. LaMar, *J. Amer. Chem. Soc.*, 92, 1806 (1970).

Synthesis and Properties of Hydridodinitrogentris(triphenylphosphine)cobalt(I) and the Related Phosphine–Cobalt Complexes

Akio Yamamoto,* Shoji Kitazume, Lyong Sun Pu, and Sakuji Ikeda

Contribution from the Research Laboratory of Resources Utilization, Tokyo Institute of Technology, Meguro, Tokyo, Japan.
Received May 29, 1970

Abstract: Hydridodinitrogentris(triphenylphosphine)cobalt(I) (**1**) was prepared from cobalt(II) and cobalt(III) acetylacetonates, organoaluminum compounds, triphenylphosphine, and molecular nitrogen. The effect of substitution of the triphenylphosphine ligands by other phosphine ligands on the infrared N_2 stretching band was studied. The nitrogen ligand coordinated to cobalt can be easily displaced reversibly by hydrogen and ammonia as shown in Figure 2. Complex **1** exhibits various chemical properties as shown in Figure 3 in agreement with its formulation as a hydride complex. Methylcobalt and ethylenecobalt complexes were also prepared in a similar manner using dimethylaluminum monoethoxide and diethylaluminum monoethoxide, respectively, and by employing an argon atmosphere. Reactions of the ethylene complex as shown in Figure 4 are consistent with its formulation as a zerovalent complex. Complex **1** catalyzes a variety of reactions such as the oxidation of triphenylphosphine, the reduction of nitrous oxide, the hydrogenation of ethylene, the dimerization and isomerization of olefins, and polymerization of vinyl compounds. The role of the cobalt–hydride bond in catalytic reactions involving olefins is discussed.

Since the discovery of nitrogen fixation under mild conditions by systems composed of transition metal compounds and reducing agents,[1] and the succeeding isolation of N_2-coordinated transition metal complexes by reaction of transition metal complexes with nitrogen compounds,[2,3] the problem of nitrogen fixation by transition metal complexes has attracted great interest.[4]

Previously we reported briefly the preparation of the N_2–cobalt complex which was the first example of the isolation of an N_2-coordinated complex prepared by a direct reaction of a transition metal complex with molecular nitrogen.[5] The complex was prepared by the reaction of cobalt(III) acetylacetonate, diethylaluminum monoethoxide, and triphenylphosphine in an atmosphere of nitrogen.

$$Co(acac)_3 + AlEt_2OEt + PPh_3 + N_2 \longrightarrow \underset{\mathbf{1}}{CoH(N_2)(PPh_3)_3}$$

We assigned the formula $Co(N_2)(PPh_3)_3$ to the complex at that time on the basis of elementary analysis, its infrared spectrum which did not exhibit a Co–H band, and a pyrolysis experiment which released 1.0 mol of N_2 and only 0.1 mol of H_2 per cobalt. Following our paper, apparently the same compound was prepared by Misono, Uchida, and Saito[6] using a similar method with triisobutylaluminum instead of diethylaluminum monoethoxide. They suggested that the N_2 complex may be a mixture of $Co(N_2)(PPh_3)_3$ and $CoH(H_2)(PPh_3)_3$. By a different method, Sacco and Rossi prepared $CoH(N_2)$-

* Address correspondence to this author.

(1) M. E. Vol'pin and V. B. Shur, *Nature (London)*, 209, 1236 (1966), and references cited therein.

(2) (a) A. D. Allen and C. V. Senoff, *Chem. Commun.*, 621 (1966); (b) A. D. Allen, F. Bottomley, R. O. Harris, V. P. Reinsalu, and C. V. Senoff, *J. Amer. Chem. Soc.*, 89, 5595 (1967); (c) A. D. Allen and F. Bottomley, *Accounts Chem. Res.*, 1, 360 (1969).

(3) J. P. Collman and J. W. Kang, *J. Amer. Chem. Soc.*, 88, 3459 (1966); J. P. Collman, M. Kubota, F. S. Vastine, J. Y. Sun, and J. W. Kang, *ibid.*, 80, 5430 (1968).

(4) For recent reviews, see (a) R. Murray and D. C. Smith, *Coord. Chem. Rev.*, 3, 429 (1968); (b) K. Kuchynka, *Catal. Rev.*, 3, 111 (1969); (c) G. H. Olive and S. Olive, *Angew. Chem.*, 81, 679 (1969); (d) references cited in a paper by T. Ito, S. Kitazume, A. Yamamoto, and S. Ikeda, *J. Amer. Chem. Soc.*, 92, 3011 (1970); (e) T. Ito and A. Yamamoto, *Yuki Gosei Kagaku Kyokai Shi*, 28, 598 (1970); (f) Yu. G. Borod'ko and A. E. Shilov, *Usp. Khim.*, 38, 761 (1969).

(5) A. Yamamoto, S. Kitazume, L. S. Pu, and S. Ikeda, *Chem. Commun.*, 79 (1967).

(6) A. Misono, Y. Uchida, and T. Saito, *Bull. Chem. Soc. Jap.* 40, 700 (1967); A. Misono, Y. Uchida, T. Saito, and K. M. Song, *Chem. Commun.*, 419 (1967).